Electronic Supplementary Information

Hierarchical Copper Nanostructures Synthesized on Microparticles for Improved Photothermal Conversion in Photonic Sintering of Copper-Based Printed Electrodes

Jae-Won Lee [a,b], Juhee Kim [b,d], Ji Hye Kwak [c], Jung Hoon Kim [b], Sooyeon Jeong [b], Joong Tark Han [b,f], Geon-Woong Lee [b], Kang-Jun Baeg [d], Kyong-Soo Hong [e], Imjeong H.-S Yang [a*], Hee Jin Jeong [b,f*]

[a] *Department of Physics, Pusan National University, Busan 46241, South Korea*

[b] *Nano Hybrid Technology Research Center, Creative and Fundamental Research Division, Korea Electrotechnology Research Institute (KERI), Changwon 51543, South Korea*

[c] *Electrical Environment Research Center, Power Grid Research Division, Korea Electrotechnology Research Institute (KERI), Changwon 51543, South Korea*

[d] *Department of Nanotechnology Engineering, Pukyong National University, Busan 48513, South Korea*

[e] *Busan Center, Korea Basic Science Institute (KBSI), Busan 46742, South Korea*

[f] *Department of Electro-Functionality Material Engineering, University of Science and Technology (UST), Changwon 51543, South Korea*

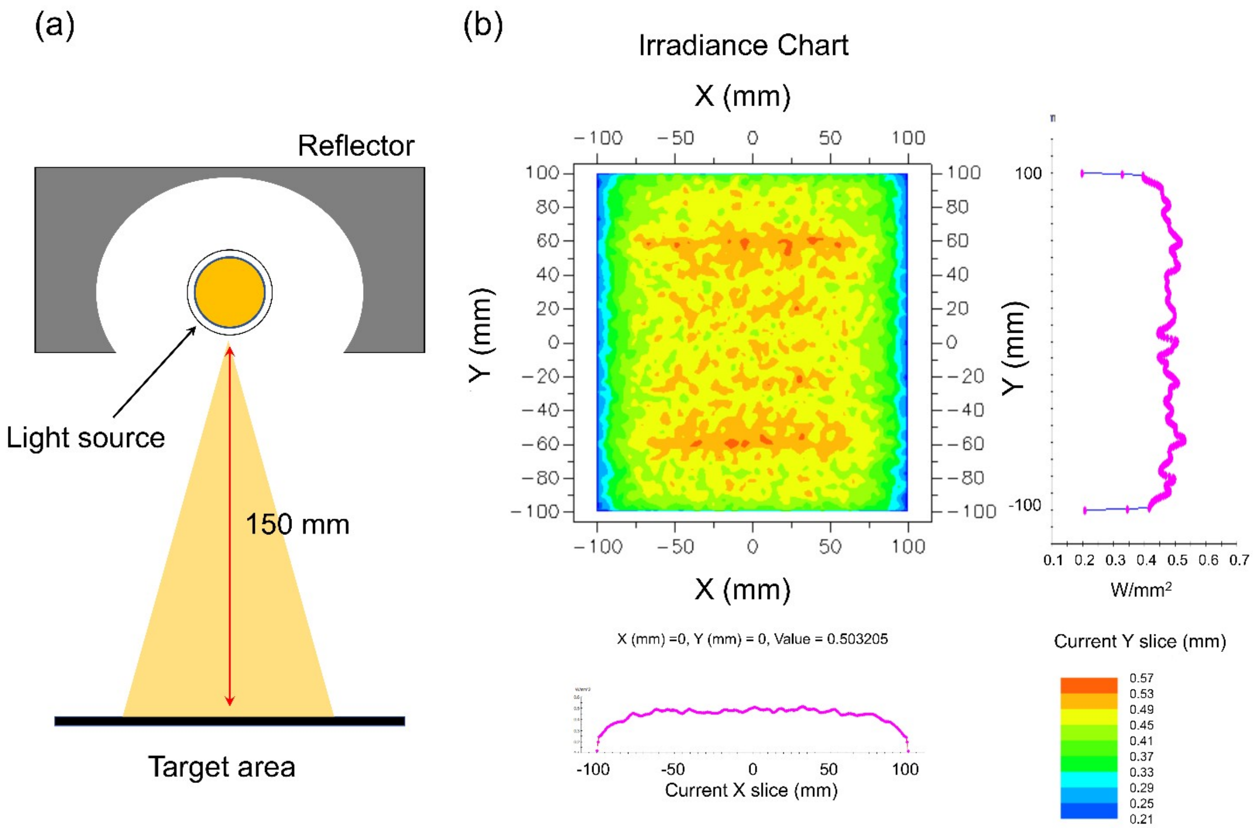

Fig S1. (a) Target specification of the xenon flash lamp. (b) Illuminance simulation of the elliptical reflector. 200 mmx200 mm receiver.

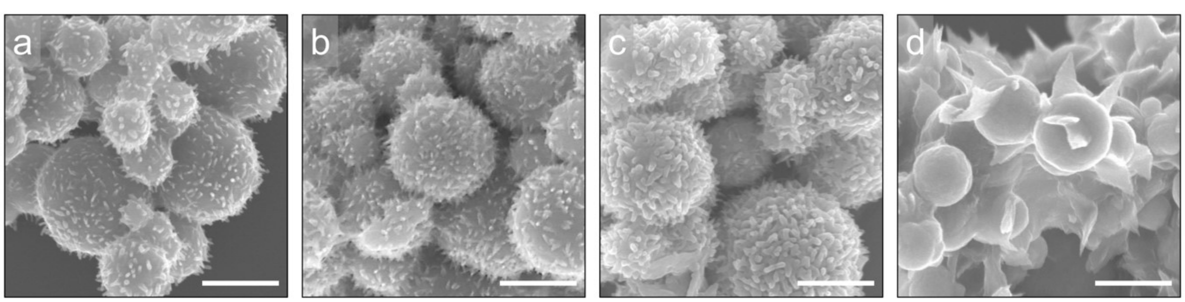

Fig S2. FE-SEM images of HN-Cu μPs obtained with different EDA content: (a) 0.5 ml, (b) 2.0 ml, (c) 5.0 ml, and (d) 5.0 ml or more. The scale bar represents 500 nm.

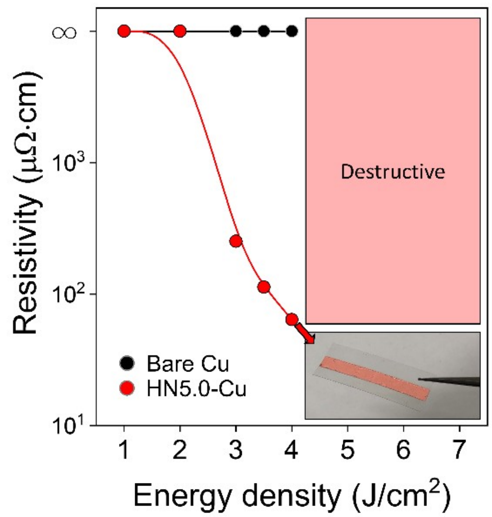

Fig S3. IPL energy density dependences of electrical resistivity for bare Cu and HN5.0-Cu sintered patterns printed on PET films. Destructive patterns were observed at the energy densities over 4 J/cm2 due to the distortion of the PET films.

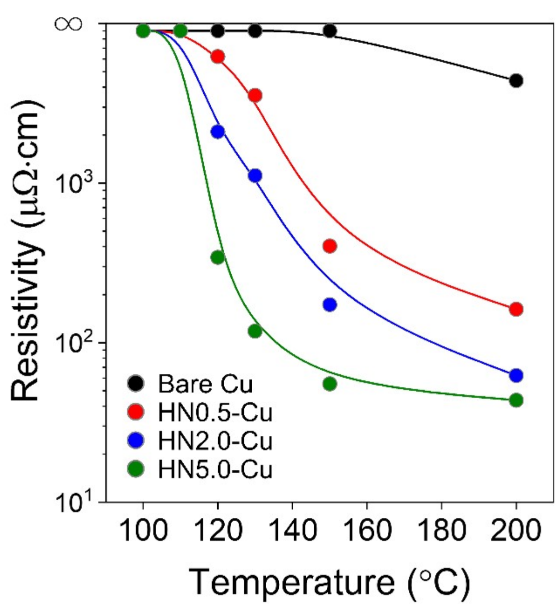

Fig S4. Electrical resistivity changes of printed bare Cu μP patterns and HN-Cu μP patterns sintered by thermal sintering.

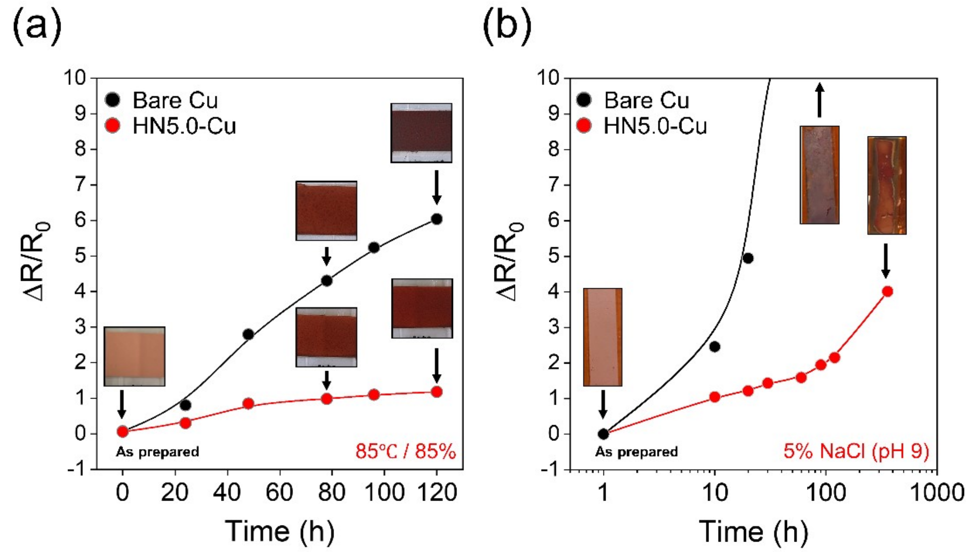

Fig. S5. Normalized resistance variations for the bare Cu and HN5.0-Cu sintered patterns during the chemical stability tests under (a) 85℃/RH85% and (b) 5% NaCl (pH 9) conditions.

In the temperature and humidity test, high temperature (85℃) and high relative humidity (RH85%) are applied simultaneously to the bare Cu and HN5.0-Cu sintered patterns for 120 hours. After the test for 120 hours, the normalized resistance varied, with values of 6.04 and 1.18 for the bare-Cu and HN5.0-Cu sintered patterns, respectively. Also, in the salt spray test (5% NaCl, pH9), the electrical performance degradation and corrosion rate of the HN5.0-Cu sintered pattern were far lower than those of the bare-Cu sintered pattern. These chemical stability tests showed that HN5.0-Cu sintered patterns had higher oxidation resistance and lower corrosion rate due to its high densification levels and uniformly sintered morphologies than the bare Cu sintered patterns.

Strategy	Energy density (J cm^{-2})	Number of pulses	Resistance (μΩ cm)	Substrate	Reference
Cu microparticles	4	5	9.54	PI	1
Cu microparticles/ Cu nanoparticles	12.5	1	72.8	PI	2
Bimodal Cu nanoparticles	6	5	5.68	PI	3
CuO nanoparticles	11.7	1	9	Silica coated PET	4
Cu nanoparticles/ CuO nanoparticles	3.08	1	70	PI	5
Cu/Cu2O precursor	17.23	10	94	PET	6
Cu nanoparticles/Cu MOD	2.7 and 2.9	1	18.2	PI	7
Cu precursor/nanoparticles (CPN)	5.17	1	12.2	PI	8
Cu nitrate hydroxide	12.8	40	125	Glass	9
Hierarchical nanostructured Cu microparticles	7	1	16	PI	This work

Table S1. The comparison of previously reported works about IPL sintering of Cu based-patterns with respect to Cu filler type, IPL sintering conditions, and electrical performance.

References

1 J.-W. Lee, J. H. Kwak, J. Kim, S. Jeong, J. H. Park, S. Y. Jeong, S. H. Seo, J. T. Han, G.-W. Lee, K.-J. Baeg, I. H.-S. Yang, H. J. Jeong, *Adv. Mater. Interfaces*, 2021, **8**, 2100769.
2 S.-J. Joo, H.-J. Hwang, H.-S. Kim, *Nanotechnology*, 2014, **25**, 265601.
3 M.-H. Yu, S.-J. Joo, H.-S. Kim, *Nanotechnology*, 2017, **28**, 205205.
4 C. Paquet, R. James, A. J. Kell, O. Mozenson, J. Ferrigno, S. Lafrenière, P. R. L. Malenfant, *Organic Electronics*, 2014, **15**, 1836.
5 W.-Y. Chung, Y.-C. Lai, T. Yonezawa, Y.-C. Liao, *Nanomaterials*, 2019, **9**, 1071.
6 R. Dharmadasa, M. Jha, D. A. Amos, T. Druffel, *ACS Appl. Mater. Interfaces*, 2013, **5**, 13227.
7 B. Deore, C. Paquet, A. J. Kell, T. Lacelle, X. Liu, O. Mozenson, G. Lopinski, G. Brzezina, C. Guo, S. Lafrenière, P. R. L. Malenfant, *ACS Appl. Mater. Interfaces*, 2019, **11**, 38880.
8 Y.-R. Jang, R. Jeong, H.-S. Kim, S. S. Park, *Scientific Reports*, 2021, **11**, 14551.
9 G. L. Draper, R. Dharmadasa, M. E. Staats, B. W. Lavery, T. Druffel, *ACS Appl. Mater. Interfaces*, 2015, **7**, 16478.